GENERATION AND DETECTION OF ULTRA-FAST X-RAY PULSES

Research Institute for Nuclear Problems

BSU

Alexander Lobko

Institute for Nuclear Problems

Belarusian State University

Minsk, Belarus

ISMART Intl Conference

(12-16 October 2014) Minsk, Belarus

Motivation

Currently the production and application of ultra-fast (sub-ps) x-ray pulses is the research area under the active development.

Approaches include laser-plasma sources producing short pulses of *Bremsstrahlung* due to interaction of ionized electrons; Compton scattering of short laser pulses on relativistic electrons from external accelerator; x-rays from laser-plasma accelerated electrons passing through periodically distributed media such as single crystal lattices, multi-layer x-ray mirrors or periodic nanostructures.

Classical and plasma acceleration

RF Cavity

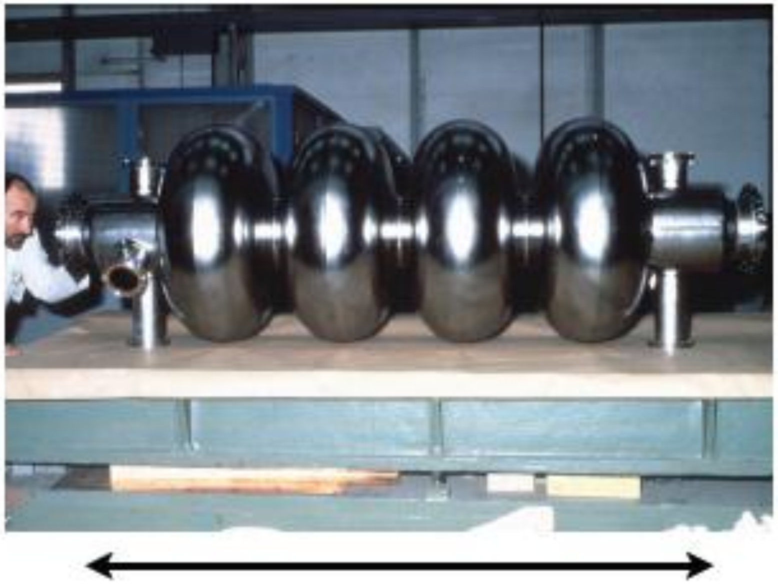

1 m => 100 MeV Gain

Electric field < 100 MV/m

Plasma Cavity

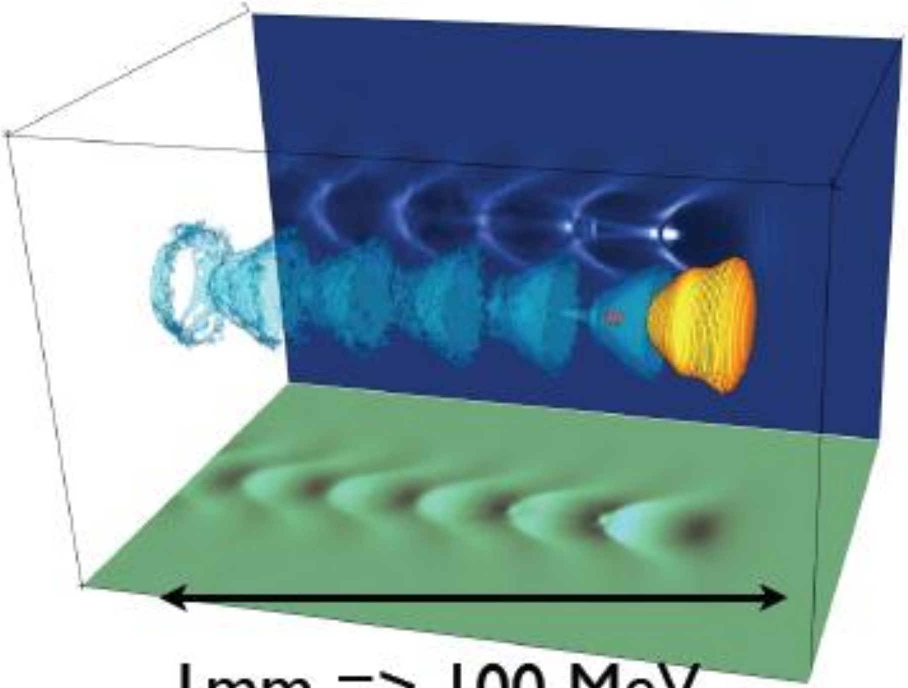

1mm => 100 MeV

Electric field > 100 GV/m

V. Malka *et al.*, Science **298**, 1596 (2002)

Evaluation of electric field at plasma wave

$$E \cong \alpha (n_e)^{\frac{1}{2}} \, [V \cdot \, cm^{-1}]$$

where

$\alpha = \delta n / n_e$ - plasma wave amplitude

$n_e = 10^{17} \, cm^{-3}$

$\alpha \approx 0.3$

$$E \sim 10^8 \, V/cm$$

Laser pulse and plasma wave

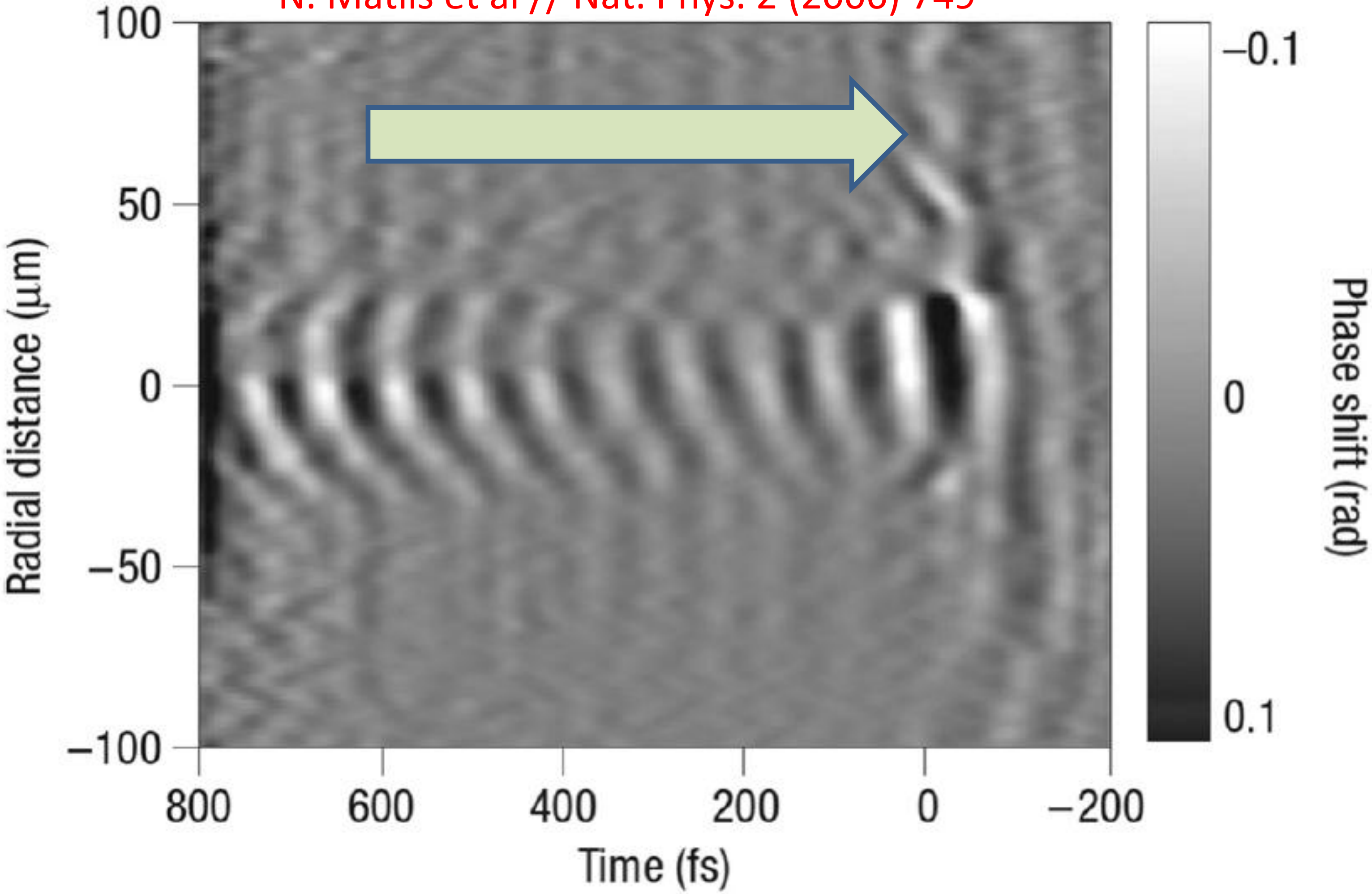

N. Matlis et al // Nat. Phys. 2 (2006) 749

The maximum amplitude of the plasma wave was measured to be in the range **20%–60%** [C. E. Clayton at al // Phys. Rev. Lett. 81 (1998) 100)].

Chirped pulse amplification (CPA)

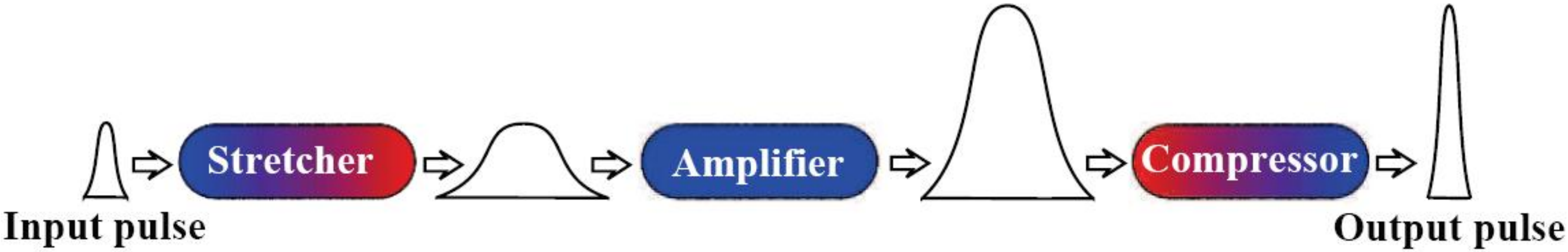

Before the invention of the CPA in 1985, laser pulses could be focused only in the two transverse dimensions by corresponding sets of lenses. The CPA technology has allowed the compression of the laser pulses in the third, longitudinal dimension, and this technological breakthrough has immediately led to a jump in the achievable powers and focused intensities.

The Petawatt shots, where an adaptive mirror has been employed, have resulted in the focal intensity

$$I = 10^{21}\ W \cdot cm^{-2}$$

Now, three classes of laser amplifiers – CPA based on Ti-Sa, CPA based on Neodymium glass, and Optical Parametric CPA based on DKDP crystals can deliver approximately the same level of power, **about 1.0 PW**.

Chirped pulse amplification (CPA)

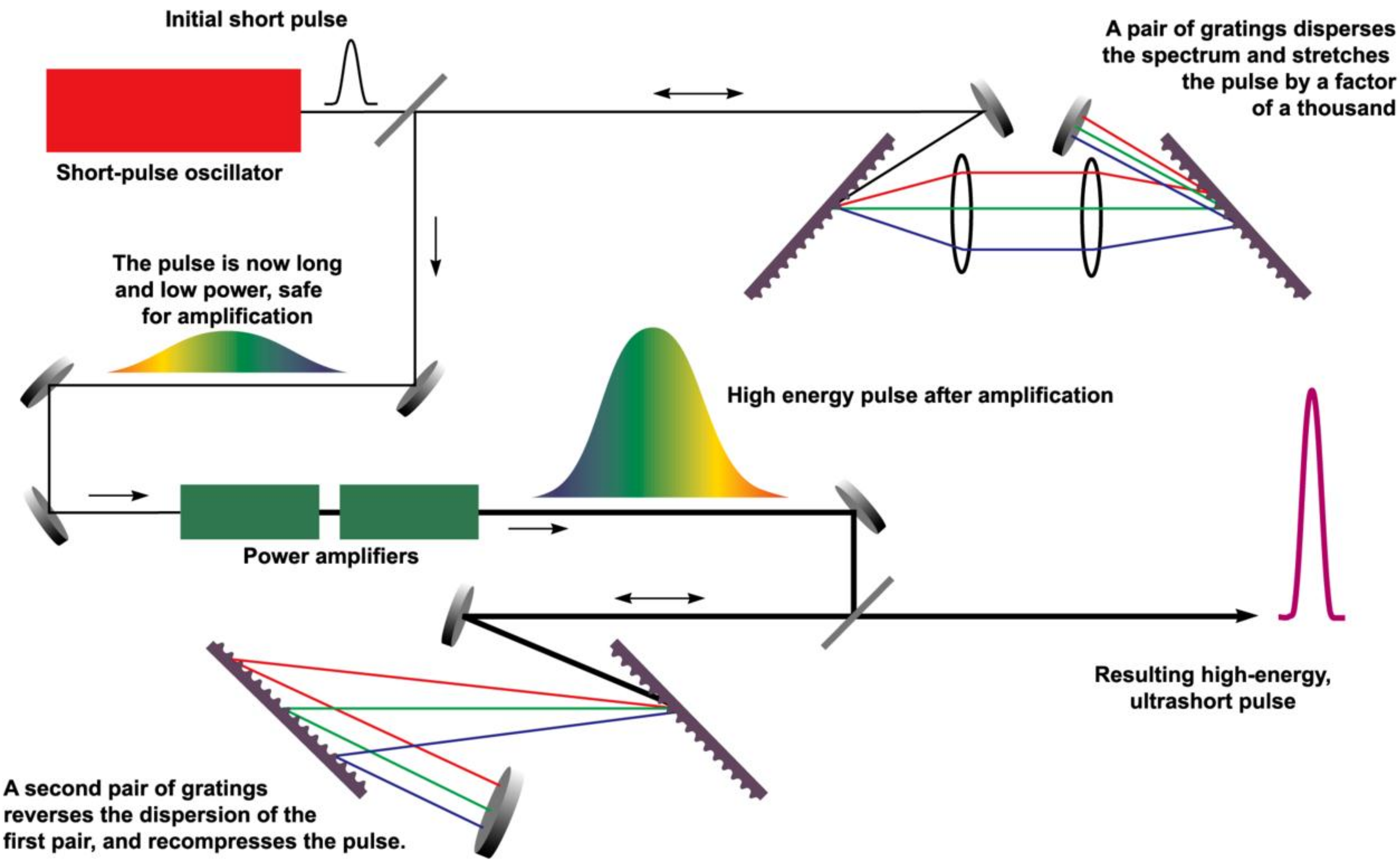

Examples of lasers at operation

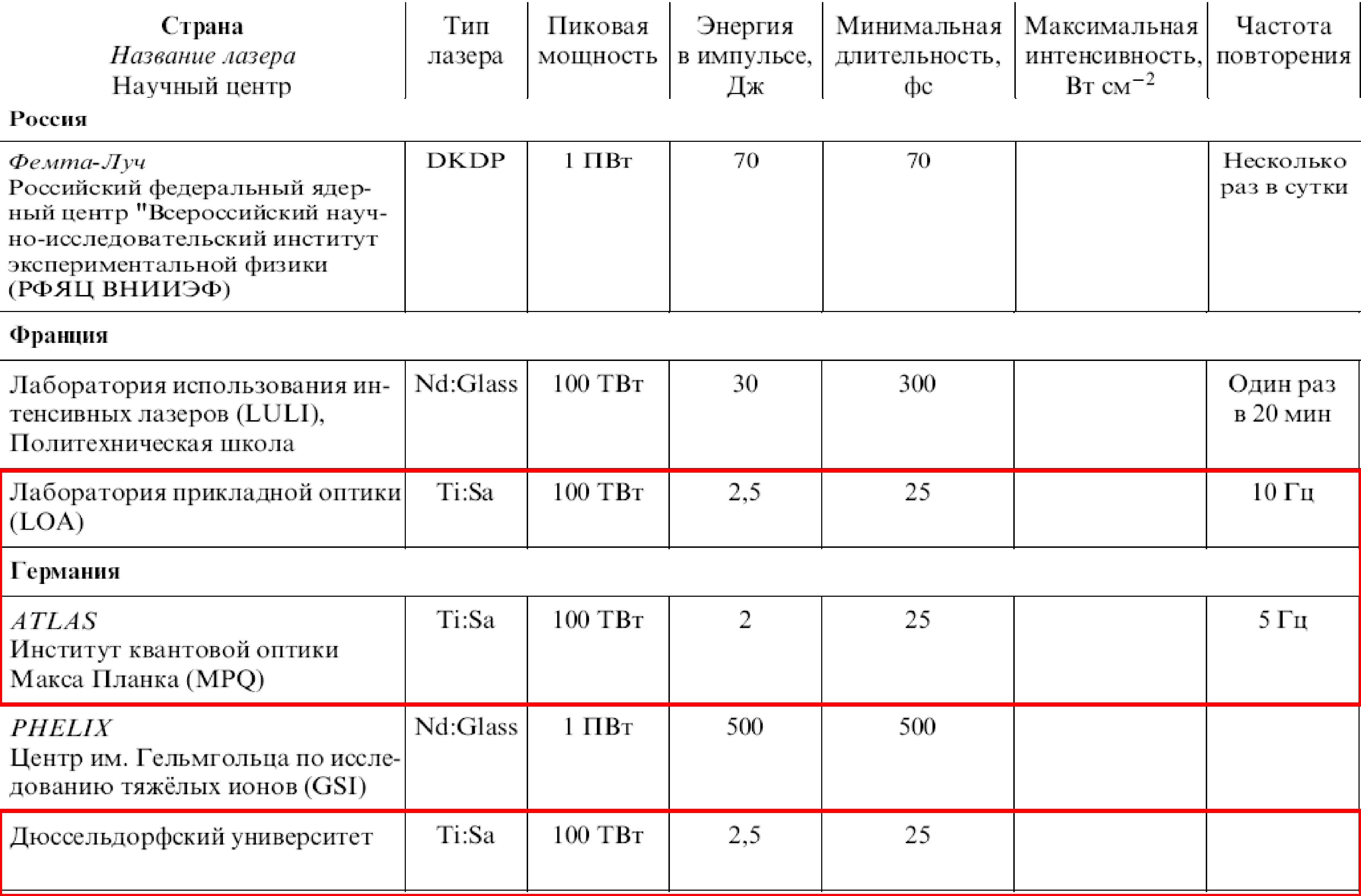

Страна *Название лазера* Научный центр	Тип лазера	Пиковая мощность	Энергия в импульсе, Дж	Минимальная длительность, фс	Максимальная интенсивность, Вт см$^{-2}$	Частота повторения
Россия						
Фемта-Луч Российский федеральный ядерный центр "Всероссийский научно-исследовательский институт экспериментальной физики (РФЯЦ ВНИИЭФ)	DKDP	1 ПВт	70	70		Несколько раз в сутки
Франция						
Лаборатория использования интенсивных лазеров (LULI), Политехническая школа	Nd:Glass	100 ТВт	30	300		Один раз в 20 мин
Лаборатория прикладной оптики (LOA)	Ti:Sa	100 ТВт	2,5	25		10 Гц
Германия						
ATLAS Институт квантовой оптики Макса Планка (MPQ)	Ti:Sa	100 ТВт	2	25		5 Гц
PHELIX Центр им. Гельмгольца по исследованию тяжёлых ионов (GSI)	Nd:Glass	1 ПВт	500	500		
Дюссельдорфский университет	Ti:Sa	100 ТВт	2,5	25		

Laser-induced ionization

For the hydrogen atom, the binding electric field is given (in SI units) by

$$E_b = \frac{e}{4\pi\epsilon_0 a_B^2} \approx 5.1 \times 10^9 \frac{V}{cm}$$

$$I_i = \frac{\epsilon_0 c E_b^2}{2} \approx 3.51 \times 10^{16} \frac{\mathrm{W}}{\mathrm{cm}^2}$$

This is the intensity at which any target material will be ionized solely by the laser electric field

In fact, with laser intensities exceeding $\boxed{\sim 10^{10}\,\mathrm{W/cm^2}}$ the photon density is high enough so that enables the multi-photon ionization process

Relativistic laser intensity

$$I_0\lambda^2 = \xi_{\mathrm{pol}} \left[1.37 \times 10^{18} \, \frac{\mathrm{W}}{\mathrm{cm}^2} \mu\mathrm{m}^2 \right] a_0^2$$

where $a_0 = \frac{v_{max}}{c} = eA_0/m_e c^2$ normalized vector amplitude

The maximum kinetic energy of the electron can be written as

$$\hat{E}_{\mathrm{kin}} = \frac{a_0^2}{2} m_e c^2$$

Focused laser with a normalized amplitude of $a_0 > 1$ is commonly referred to as ***relativistic***.

Motion of an electron in the laser field

$$x(\tau) = \frac{ca_0^2}{4}\left(\tau + \frac{1}{2\omega}\sin(2\omega\tau)\right)$$

$$z(\tau) = \frac{ca_0}{\omega}\sin(\omega\tau)$$

1. The transverse motion in z, caused by the electric field of the laser, is solely oscillatory with its amplitude depending linearly on a_0.

2. The longitudinal motion in x (the laser propagation direction), caused by the $v \times B$ term of the Lorentz equation, has a linear term in τ in addition to the oscillatory term, which also depends quadratically on a_0.

External injection

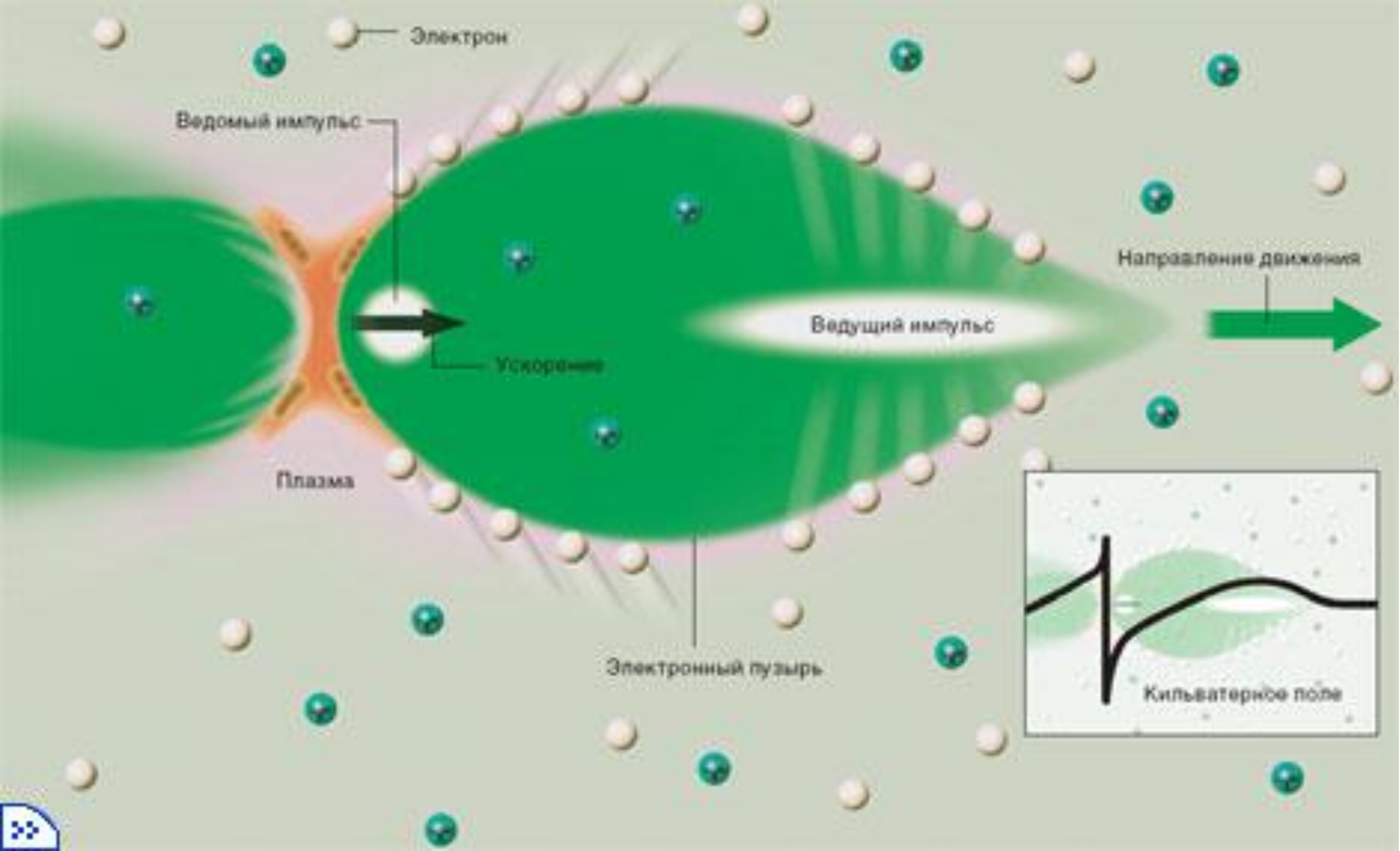

Supersonic jet target schematics

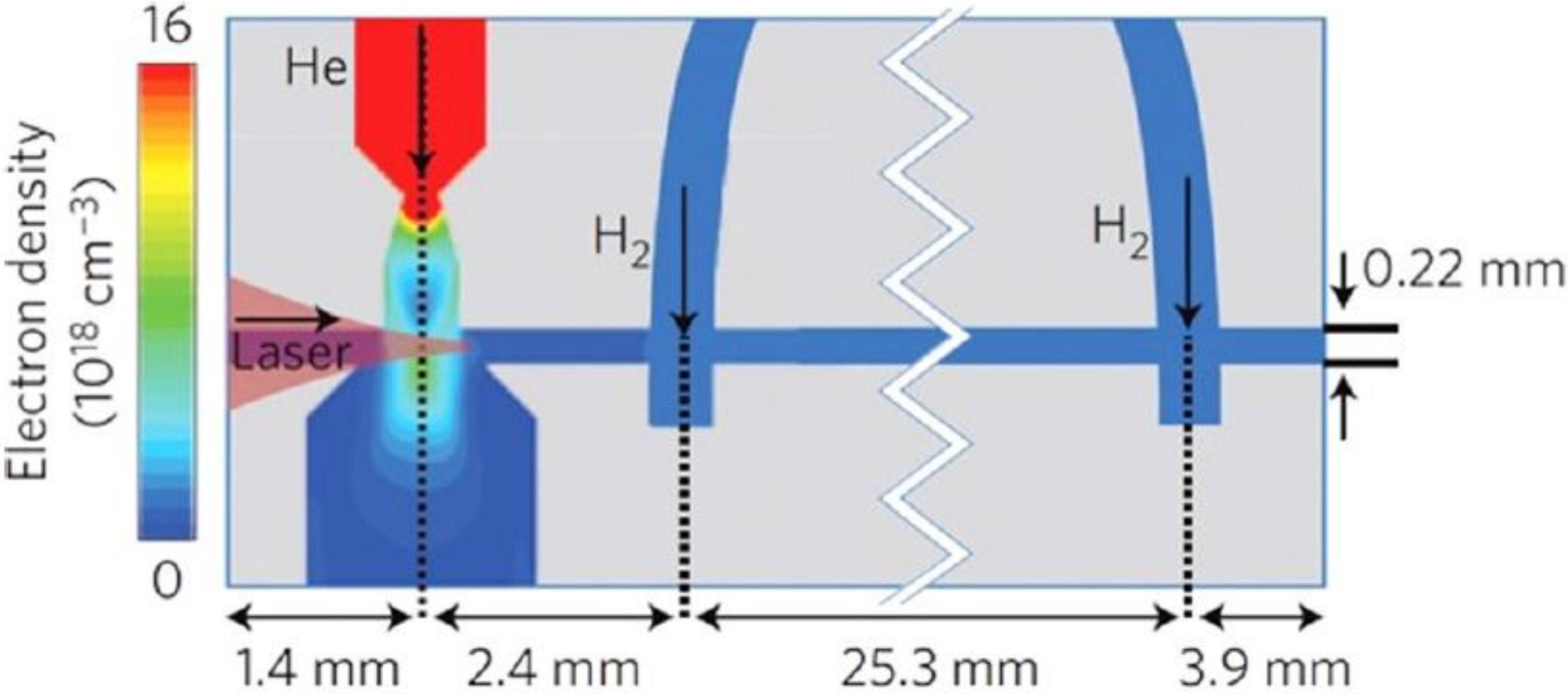

One of the solutions to control electron injection is injection at <u>downward</u> density ramp with a density gradient scale length greater than the plasma wavelength.

Beam quality

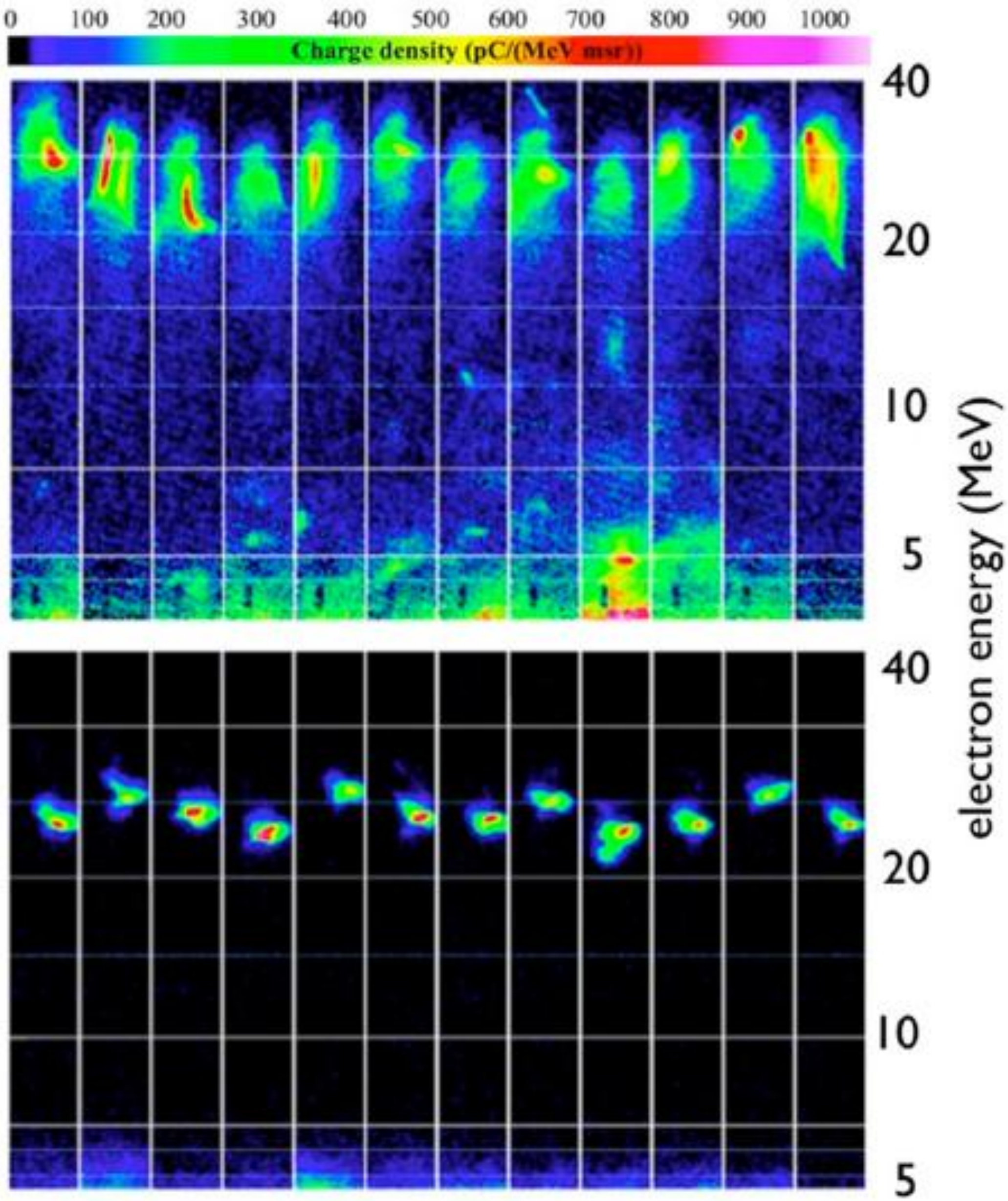

Comparison of self-injection (top) and injection at a density transition (bottom)

Bubble regime-transverse injection

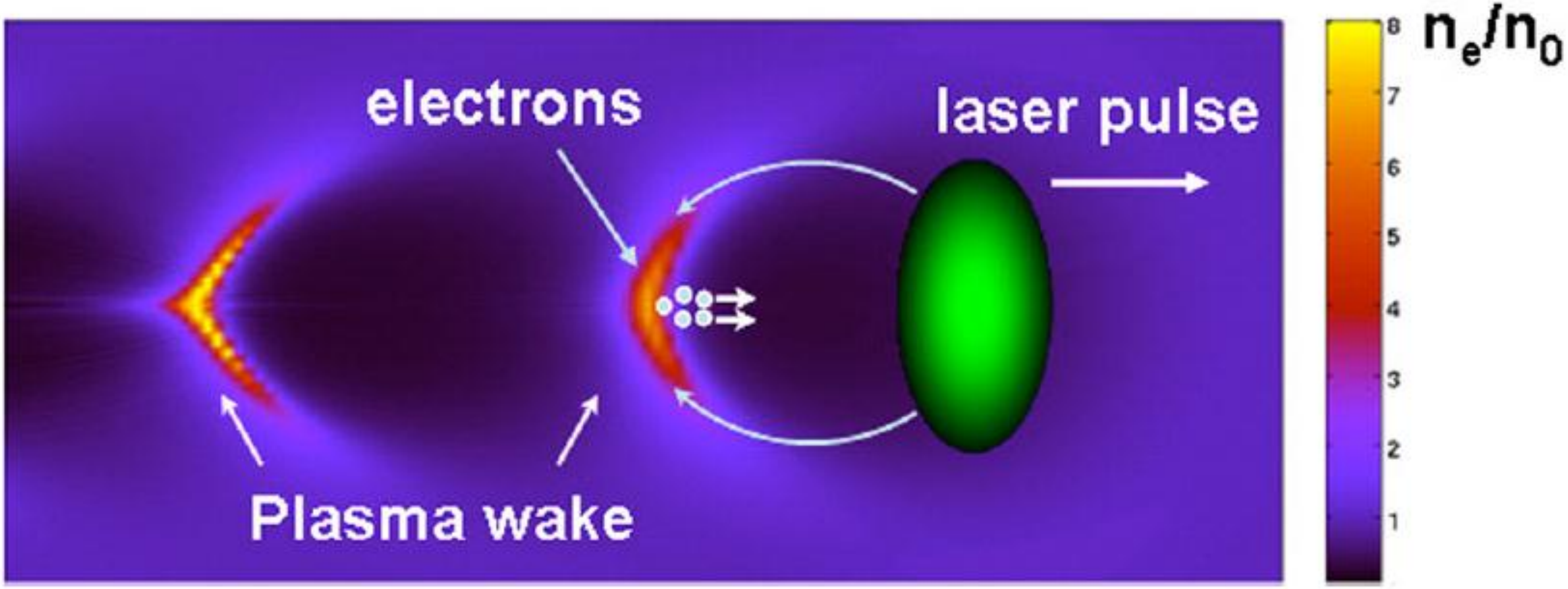

The laser pulse that propagates from left to right, expels electrons on his path, forming a positively charged cavity. The radially expelled electrons flow along the cavity boundary and collide at the bubble base, before being accelerated behind the laser pulse. The fact that electrons are trapped behind the laser, where they no more interact with the laser field, contributes to improving of quality of the electron beam.

Transition between acceleration regimes

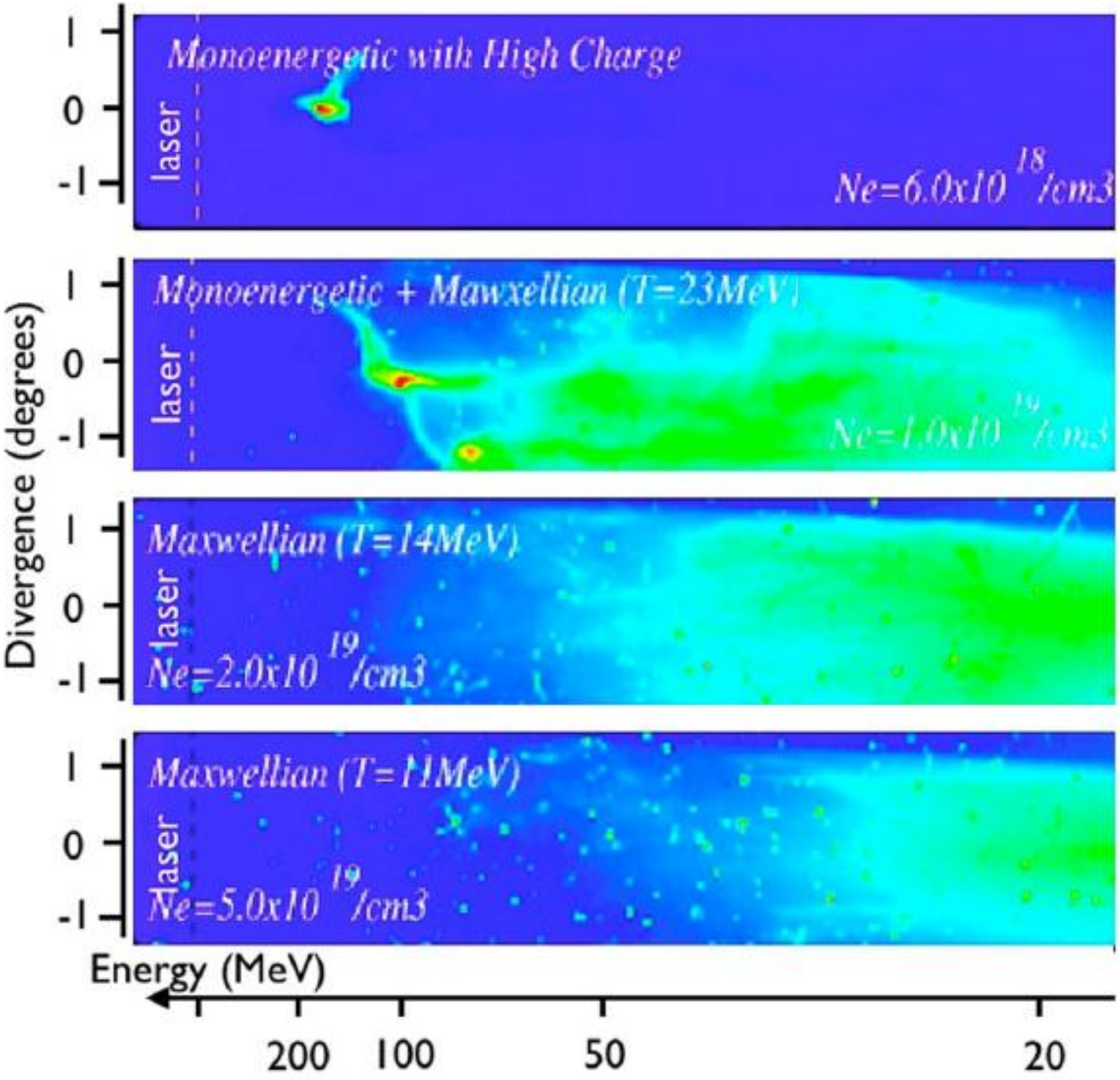

Electron beam distribution for different plasma densities showing the transition from the self modulated laser wakefield and the forced laser wakefield to the bubble/blow-out regime.

Colliding laser pulses

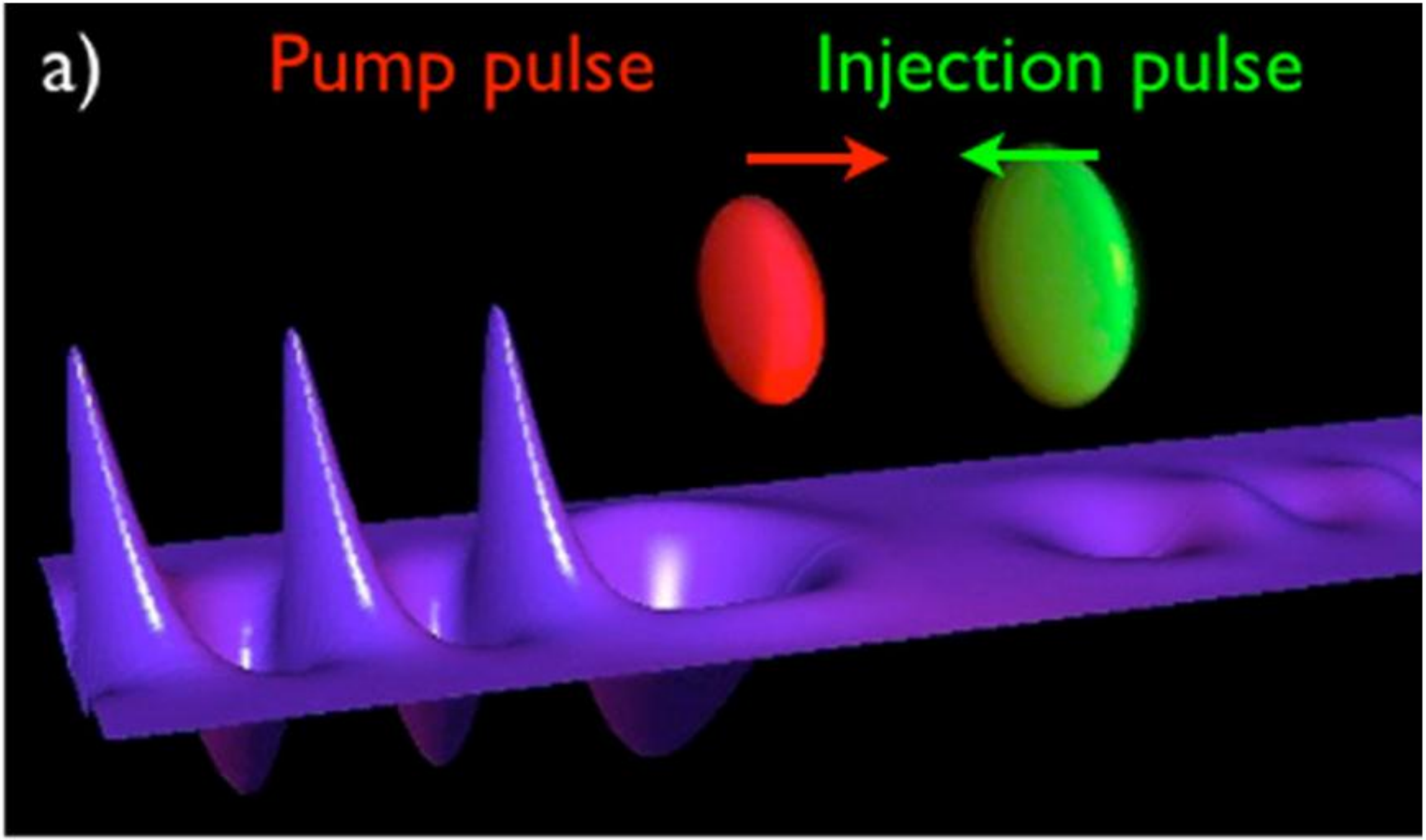

Two laser pulses propagate in opposite directions

Colliding laser pulses

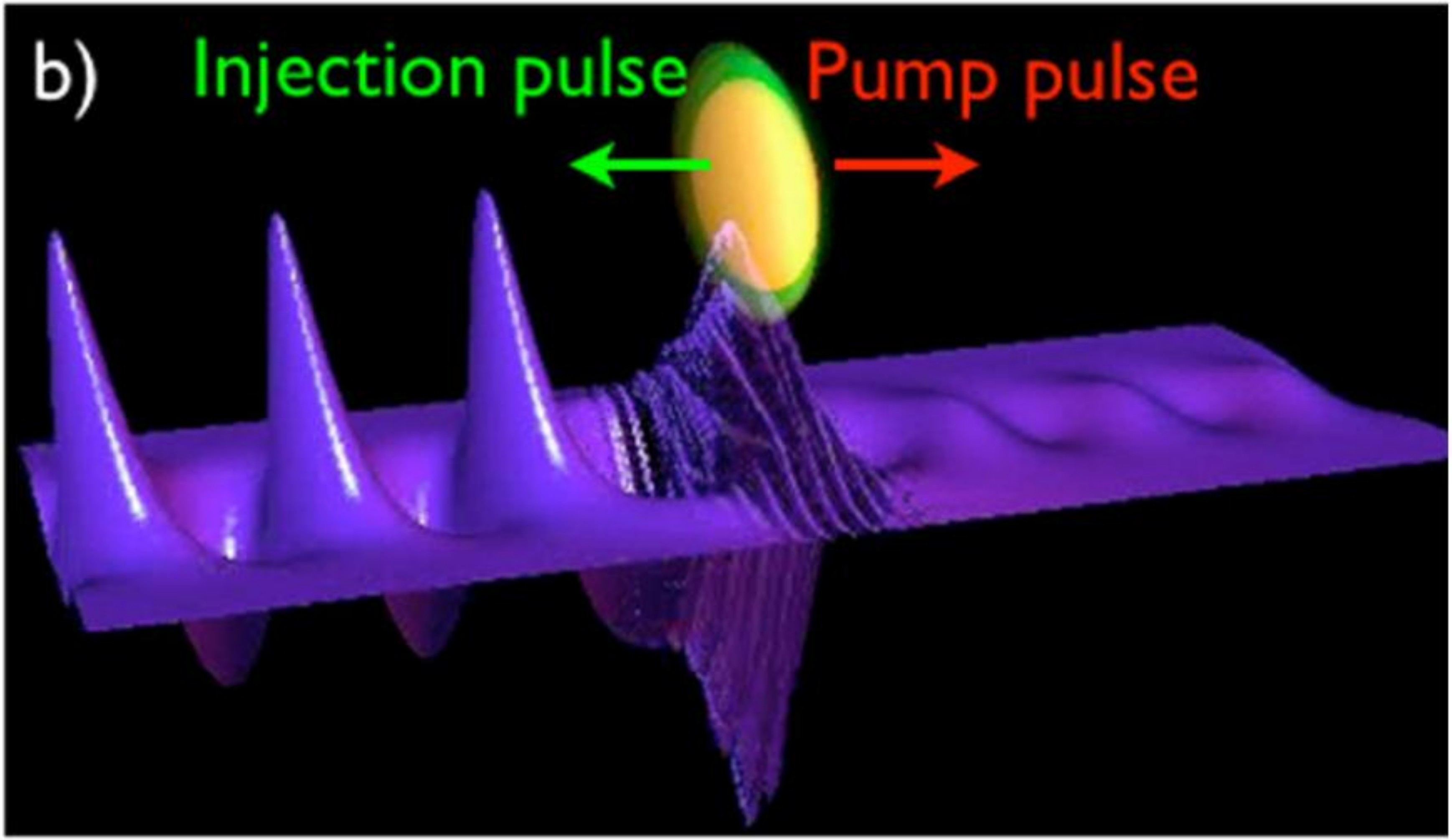

During the collision, some electrons get enough longitudinal momentum to be trapped by the relativistic plasma wave driven by the pump beam

Colliding laser pulses

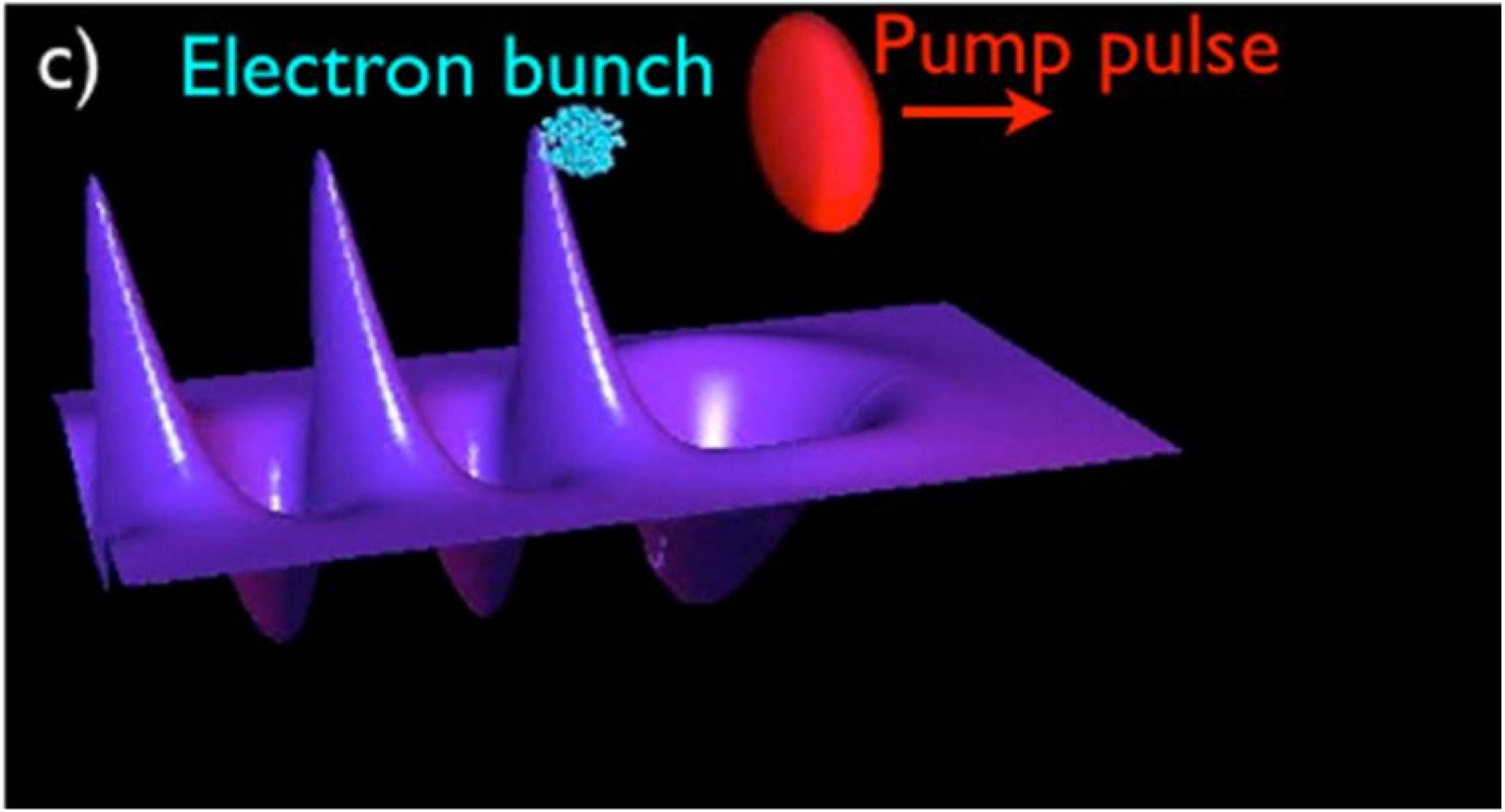

Trapped electrons are accelerated in the wake of the pump laser pulse

Experimental setup

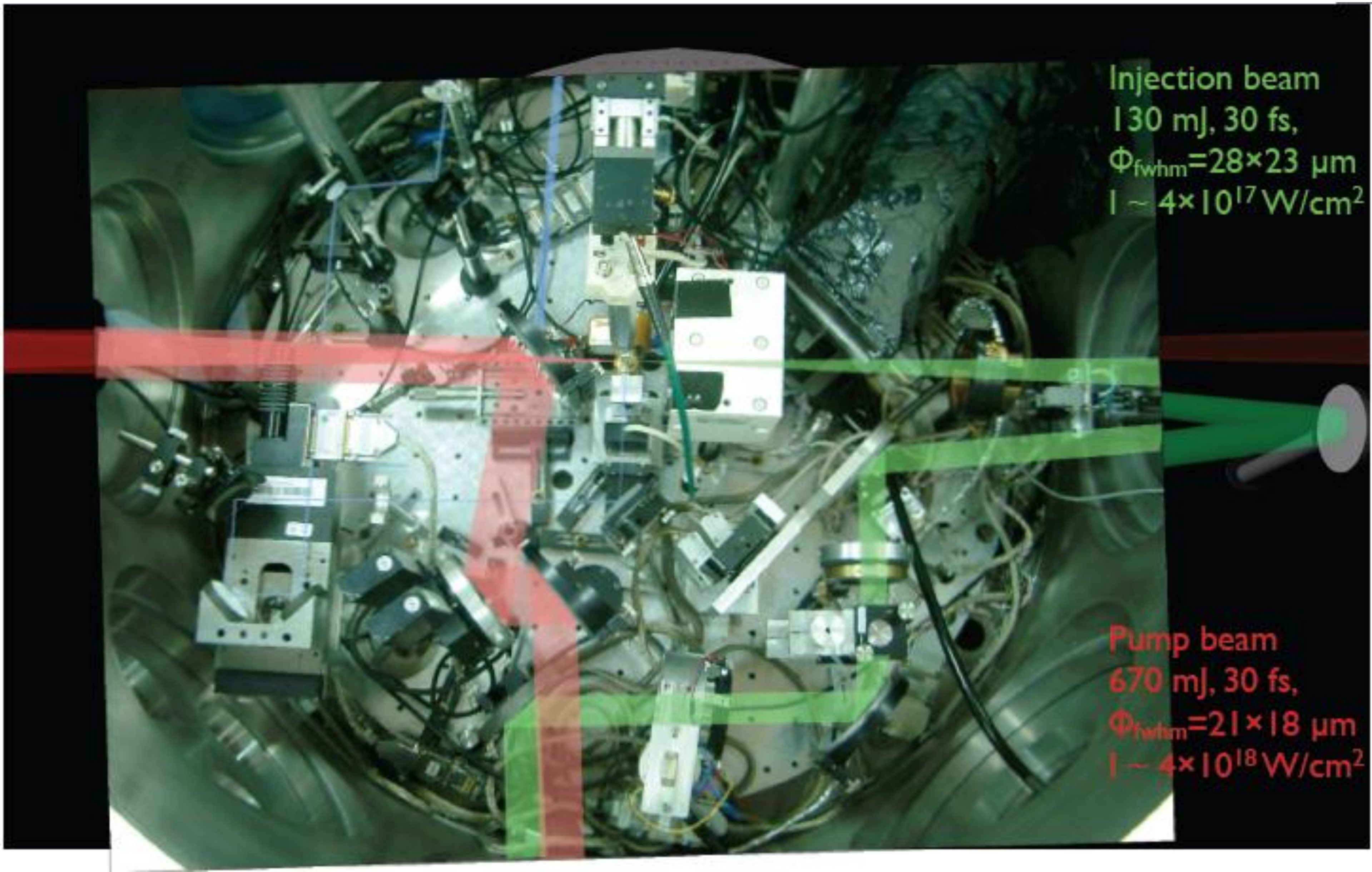

Injection beam
130 mJ, 30 fs,
$\Phi_{fwhm}=28\times23\ \mu m$
$I \sim 4\times10^{17}\ W/cm^2$

Pump beam
670 mJ, 30 fs,
$\Phi_{fwhm}=21\times18\ \mu m$
$I \sim 4\times10^{18}\ W/cm^2$

Beam energy tunability

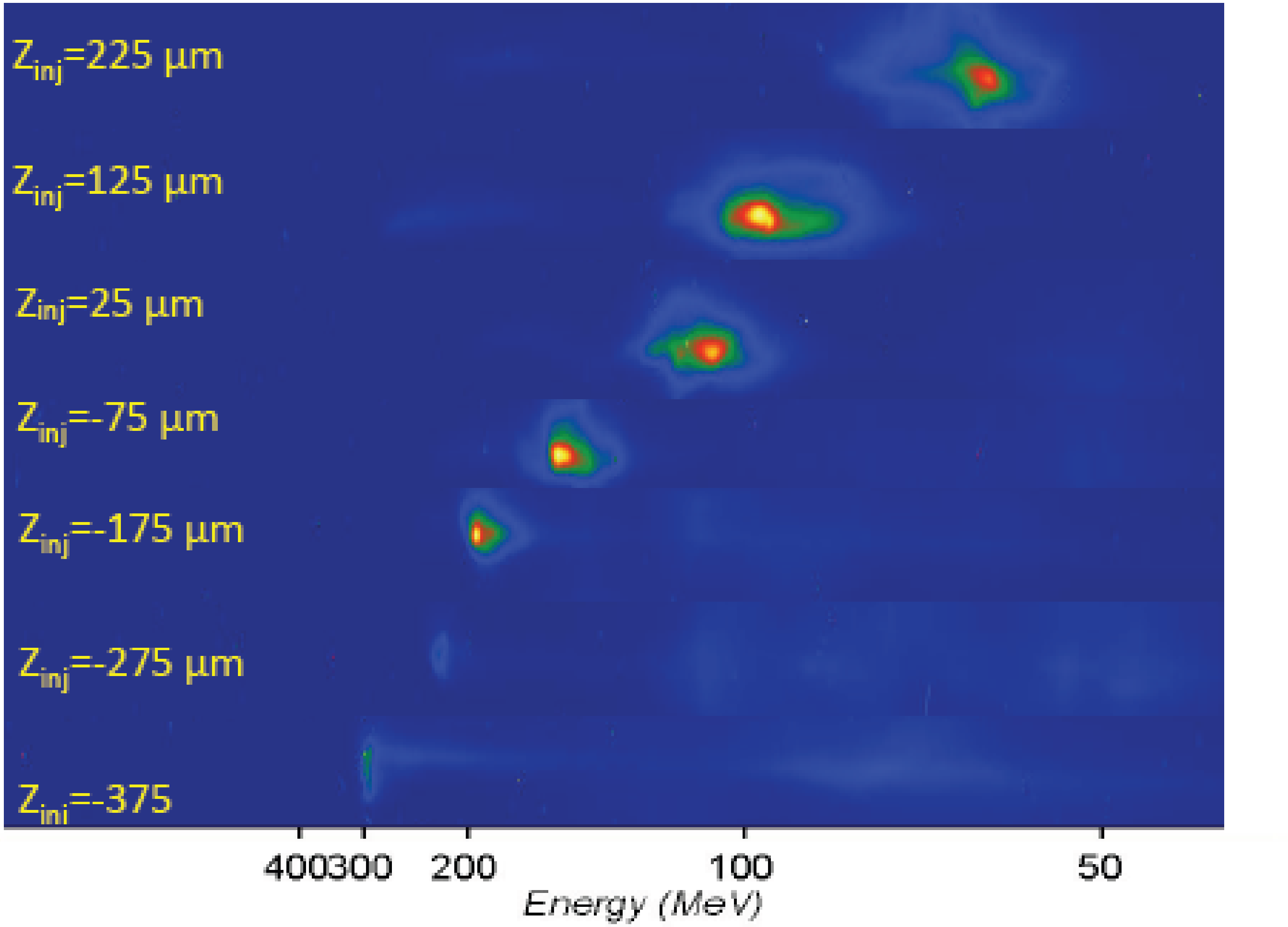

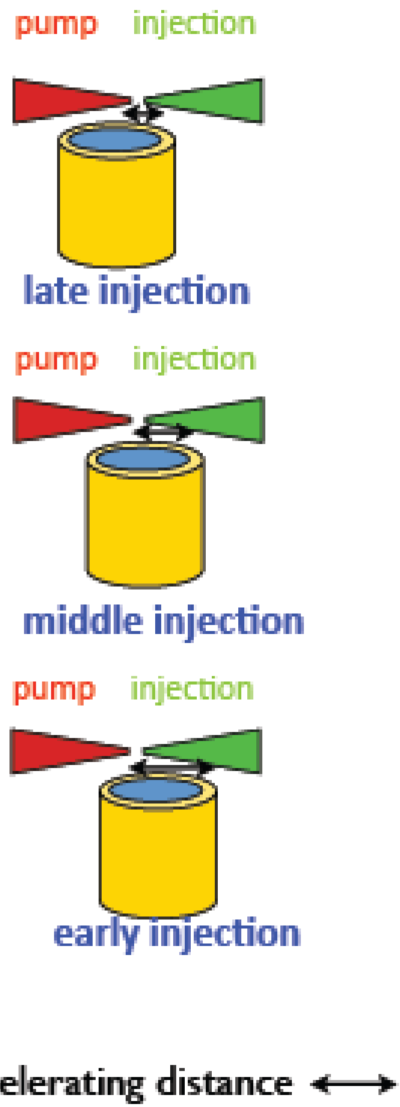

J. Faure *et al.*, Nature **444**, 737 (2006)

Beam energy spread

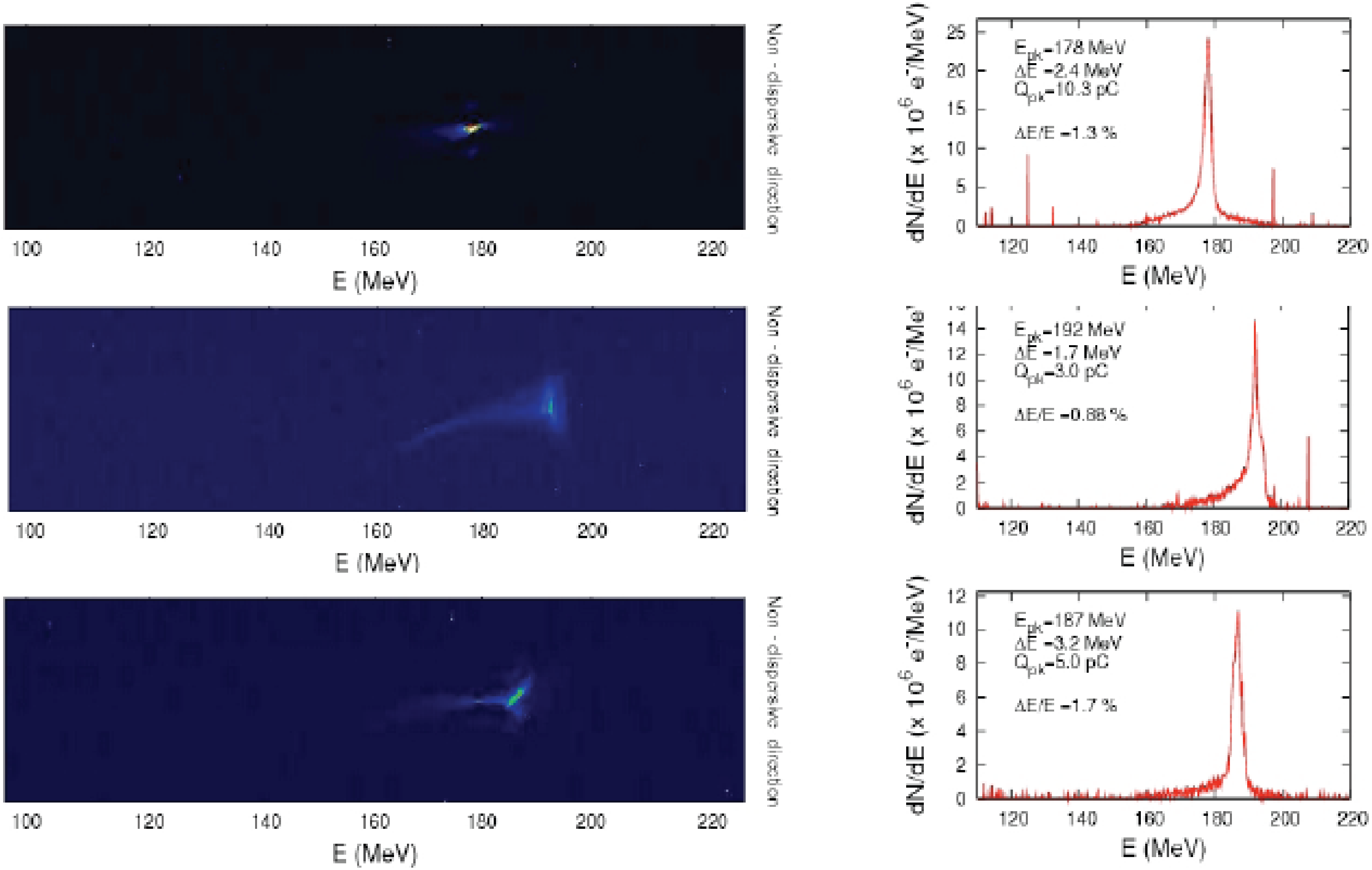

C. Rechatin *et al.*, Phys. Rev. Lett. **102**, 194804 (2009)

Beam properties

Good beam quality & Monoenergetic dE/E down to 1 % √

Beam is very stable √

Energy is tunable: up to 400 MeV √

Charge is tunable: 1 to tens of pC √

Energy spread is tunable: 1 to 10 % √

Ultra short e-bunch : 1,5 fs rms √

Low divergence : 2 mrad √

Low emittance[1-3] : π.mm.mrad √

[1] S. Fritzler *et al.*, Phys. Rev. Lett. **92**, 165006 (2004), [2] C. M. S. Sears *et al.*, PRSTAB **13**, 092803 (2010)
[3] E. Brunetti *et al.*, Phys. Rev. Lett. **105**, 215007 (2010)

All-optical Compton gamma-source

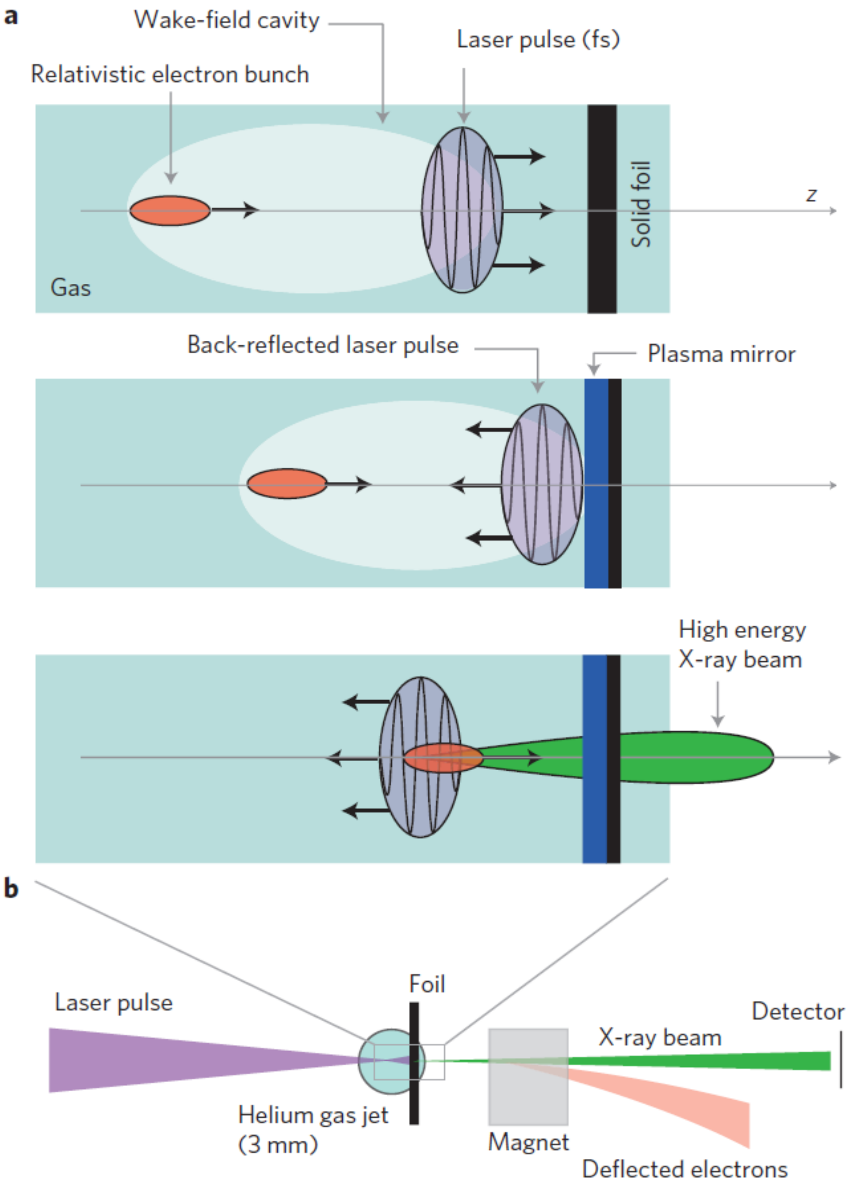

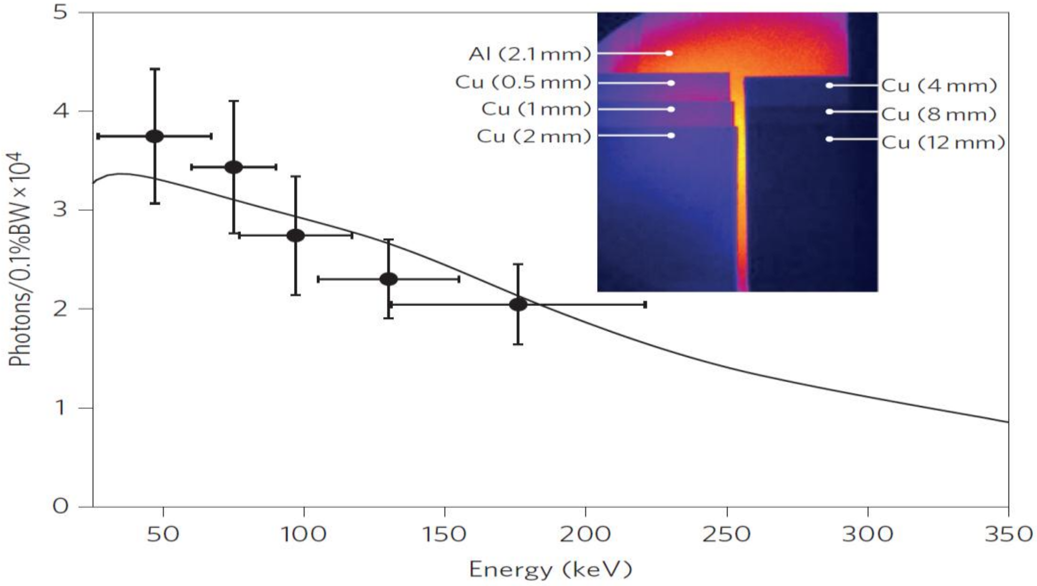

Ta Phuoc K., Corde S., Thaury C. at al. // Nature Phot. Letters. 2012.

Beam diagnostics

LANEX Fast Screens have a thin clear overcoat to resist surface abrasion and have a backing layer to eliminate curl. They incorporate as phosphor terbium-activated gadolinium oxysulfide, GdS:Tb, coated in a transparent binder.

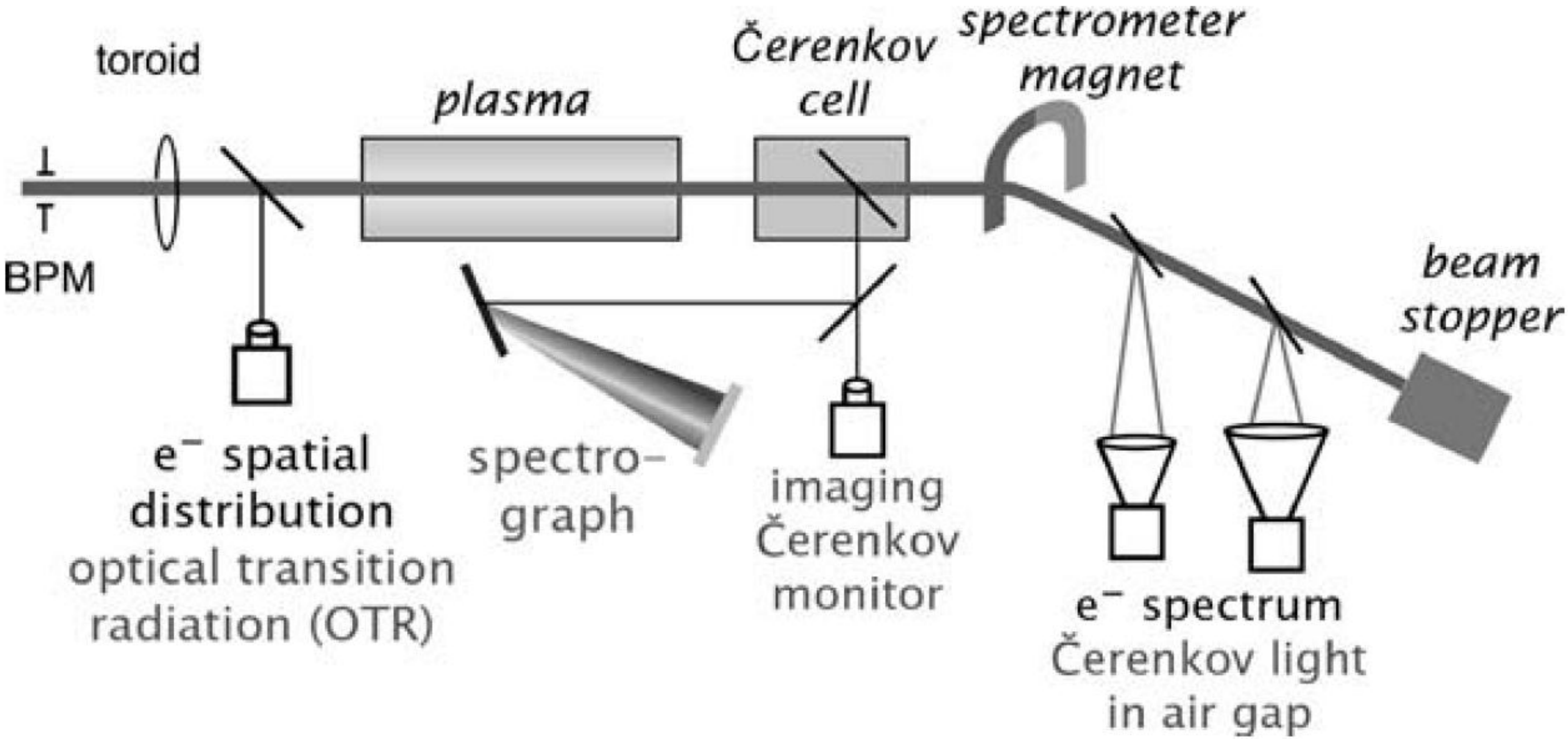

Laser-plasma interactions. Eds.: Jaroszynsky D.A., Bingham R., Cairns R.A. CRC Press, 2009. – 427 p.

CONCLUSION

Results extremely important for :

Designing future accelerators

Compact X ray source (Thomson, Compton, Betatron, or FEL)

Applications (chemistry, radiotherapy, medicine, material science, ultrafast phenomena studies, etc...)

The micron size dimensions of laser-plasma accelerating structures forms naturally ultra-short intense electron bunches resulted in ultra-short bright x-ray pulses. In other words, this research activity **demands new x-ray detection and diagnostic techniques to characterize such ultrafast bursts of radiation**.

Transient nature of these processes and small dimensional scales present challenges to x-ray measurement and metrology in the femtosecond and sub-femtosecond scale.

Thank you for attention